BROOKHAVEN
NATIONAL LABORATORY

BNL-74992-2005-CP

The normal state gap in electron doped cuprates

R.P.S.M. Lobo and N. Bontemps
Laboratoire de Physique du Solide, Ecole Superieure de Physique et Chimie Industrielles de la Ville de Paris

A. Zimmers, Y. Dagan, and R.L. Greene
Center for Superconductivity Research, Department of Physics, University of Maryland, College Park, Maryland 20742 USA.

P. Fournier
Regroupement Quebecois sur les Materiaux de Pointe and Departement de Physique, Universite de Sherbrooke, Sherbrooke, Quebec, CANADA, J1K 2R1

C.C. Homes
Department of Physics, Brookhaven National Laboratory, Upton, New York 11973, USA.

A.J. Millis
Physics Department, Columbia University, New York, New York 10027, USA.

Physics Dept., 510C, Brookhaven National Laboratory, Upton, NY 11973, USA

Physics Department

Brookhaven National Laboratory
P.O. Box 5000
Upton, NY 11973-5000
www.bnl.gov

Notice: This manuscript has been co-authored by employees of Brookhaven Science Associates, LLC under Contract No. DE-AC02-98CH10886 with the U.S. Department of Energy. The publisher by accepting the manuscript for publication acknowledges that the United States Government retains a non-exclusive, paid-up, irrevocable, world-wide license to publish or reproduce the published form of this manuscript, or allow others to do so, for United States Government purposes.

This preprint is intended for publication in a journal or proceedings. Since changes may be made before publication, it may not be cited or reproduced without the author's permission.

DISCLAIMER

This report was prepared as an account of work sponsored by an agency of the United States Government. Neither the United States Government nor any agency thereof, nor any of their employees, nor any of their contractors, subcontractors, or their employees, makes any warranty, express or implied, or assumes any legal liability or responsibility for the accuracy, completeness, or any third party's use or the results of such use of any information, apparatus, product, or process disclosed, or represents that its use would not infringe privately owned rights. Reference herein to any specific commercial product, process, or service by trade name, trademark, manufacturer, or otherwise, does not necessarily constitute or imply its endorsement, recommendation, or favoring by the United States Government or any agency thereof or its contractors or subcontractors. The views and opinions of authors expressed herein do not necessarily state or reflect those of the United States Government or any agency thereof.

Printed on recycled paper

BNL-74992-2005-CP

The normal state gap in electron doped cuprates

R.P.S.M. Lobo and N. Bontemps
Laboratoire de Physique du Solide, École Supérieure de Physique et Chimie Industrielles de la Ville de Paris, CNRS UPRA0005, 10 rue Vauquelin, 75005 Paris, France

A. Zimmers, Y. Dagan, and R.L. Greene
Center for Superconductivity Research, Department of Physics, University of Maryland, College Park, Maryland 20742, USA.

P. Fournier
Regroupement Québécois sur les Matériaux de Pointe and Département de Physique, Université de Sherbrooke, Sherbrooke, Québec, CANADA, J1K 2R1

C.C. Homes
Department of Physics, Brookhaven National Laboratory, Upton, New York 11973, USA.

A.J. Millis
Physics Department, Columbia University, New York, New York 10027, USA.

ABSTRACT

The far and mid-infrared response of reduced and oxygenated $Pr_{2-x}Ce_xCuO_4$ thin films was measured from room temperature to 25 K. The reduced samples show a normal state partial gap which magnitude extrapolates to zero at a cerium concentration $0.15 < x < 0.17$ indicating the existence of a quantum critical point inside the superconducting dome. Upon oxygenation, this gap appears in a otherwise gapless $x = 0.17$ sample. The gap opening temperature changes between reduced and oxygenated materials in the same way as the changes observed in the Néel temperature allowing us to conclude for a magnetic origin for this normal state gap.

Keywords: Infrared spectroscopy, superconductivity, cuprates, strongly-correlated electron systems.

1. INTRODUCTION

The 'pseudogap' of hole doped cuprates is a partial gap at the Fermi surface opening in the normal state along the anti nodal directions.[1] As in hole doped cuprates the optical conductivity is much more sensitive to the "gapless" nodal directions,[2] there is no optical conductivity spectral weight transfer to high frequencies in the pseudogap state[3] but rather a sharp decrease of the optical scattering rate.[4]

Opposite to hole doped cuprates, a normal state gap was observed to induce a low-to-high energy spectral weight transfer in the optical conductivity of electron-doped cuprates, more specifically in $Nd_{2-x}Ce_xCuO_4$ (NCCO) non superconducting single crystals.[5,6] This gap was confirmed by ARPES measurements[7] that showed a Fermi surface composed of hole-like and electron-like pockets, expected from long range magnetic order.

In a previous paper,[8] we measured the optical conductivity of $Pr_{2-x}Ce_xCuO_4$ (PCCO) films which can be made superconducting in the underdoped regime. In contrast to Onose *et al.*'s NCCO samples,[5,6] our PCCO films showed a normal state partial gap that survives in superconducting samples. This gap closes at a quantum critical point inside the superconducting dome, consistent with transport evidence on similar samples.[9] We suggested that this gap originates from a spin density wave (SDW), consistent with ARPES.[7].

In this paper, we extend the our analysis to oxygen rich samples, upon which we present a first set of data shedding light on the possible origin of the partial normal state gap. The major effect of reduction of electron doped samples is to create the superconducting phase. In addition, reduction also moves the antiferromagnetic phase boundary to lower temperatures.[10] By comparing the optical response of reduced an oxygenated samples we show that (i) the normal state gap indeed has a magnetic origin and (ii) the effect of oxygenating the sample cannot be regarded simply as an "effective doping".

Address correspondence to lobo@espci.fr.

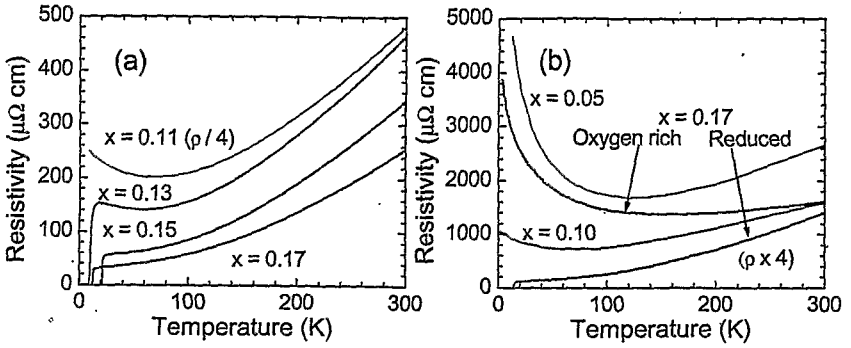

Figure 1. (a) Resistivity of the four films grown at the University of Maryland. These samples underwent a reducing thermal treatment in order to optimize T_c. Note that the resistivity of the $x = 0.11$ has been divided by 4 to fit in the same scale. (b) Resistivity of the $x = 0.17$ Sherbrooke reduced and oxygen rich films. For comparison, the resistivities of reduced $x = 0.05$ and $x = 0.10$ samples grown in the same conditions are shown. The reduced 0.17 resistivity has been multiplied by 4 for clarity.

2. EXPERIMENTAL

A first series of PCCO films were epitaxially grown by pulsed-laser deposition on $SrTiO_3$ substrates at the University of Maryland.[11] These samples have nominal Ce compositions $x = 0.11$ (not superconducting down to 4 K); $x = 0.13$ ($T_c = 15$ K); $x = 0.15$ ($T_c = 21$ K); and $x = 0.17$ ($T_c = 15$ K). All the films were thermally treated in reducing atmosphere to obtain the highest superconducting temperatures. The samples are between 3000 and 4000 Å thick and their resistivities are shown in Fig. 1 (a). All samples show the typical positive curvature observed in electron doped cuprates. For the two lowest doping samples, the resistivity goes through a minimum at a temperature that increases with decreasing doping.

Two extra films with $x = 0.17$ were grown at Sherbrooke also by pulsed-laser ablation deposition.[11,12] One of this samples was reduced to obtain $T_c = 14$ K, similar to the University of Maryland sample. The second sample was annealed in O_2 to achieve a high degree of oxygen doping.[13] This oxygenated sample did not show superconductivity down to 4 K. Figure 1 (b) shows the resistivity of both films grown at Sherbrooke as well as the resistivity of reduced films with nominal Ce contents $x = 0.05$ and $x = 0.10$. The oxygen rich 0.17 sample shows the same low temperature upturn observed in the low Ce doping compounds. Whereas the resistivity of the reduced 0.17 sample is similar to the one in panel (a), the oxygen rich material has a resistivity lying between those of reduced 0.05 and 0.10 compounds. The temperature at which the resistivity goes through a minimum, however, is higher than the one observed in the 0.05 Ce sample.

The optical reflectivity of the samples shown in Fig. 1 was measured at several temperatures from 300 K down to 25 K from 50 to 21000 cm^{-1} (Maryland series) and from 100 to 6000 cm^{-1} (Sherbrooke series). The data were collected in a Bruker IFS 66v Fourier transform spectrometer. The very far-infared (20–200 cm^{-1}) was also measured in a Bruker IFS113v at Brookhaven National Laboratory for a few samples. Panel (a) of Fig. 2 shows the measured far and mid-infrared reflectivity for all Maryland films at 300 K and 25 K. A dip in the reflectivity of the $x = 0.11$ and 0.13 appears at low temperatures around 2000 cm^{-1}. This dip can be perceived as a small bending at the lowest temperature in the $x = 0.15$ sample. No clear signature of this feature is present at the $x = 0.17$ sample. Panel (b) shows the reflectivity in the same range for the reduced and oxygen rich Sherbrooke films. The reflectivity of the University of Sherbrooke reduced $x = 0.17$ sample is similar to one measured for the sample shown in panel (a). The effect of oxygenating the sample appears as a dip in the reflectivity qualitatively similar, albeit much less deep, to the one observed in the low Cerium concentration samples of panel (a). In any case, a clear crossing of the low and high temperatures reflectivities is observed around 2500 cm^{-1}.

To describe the University of Maryland samples optical data we simulated a dielectric function that fits the reflectivity taking into account the finite thickness of the film and the optical properties of the substrate, measured in separate at all temperatures. The optical conductivity was then calculated from the obtained

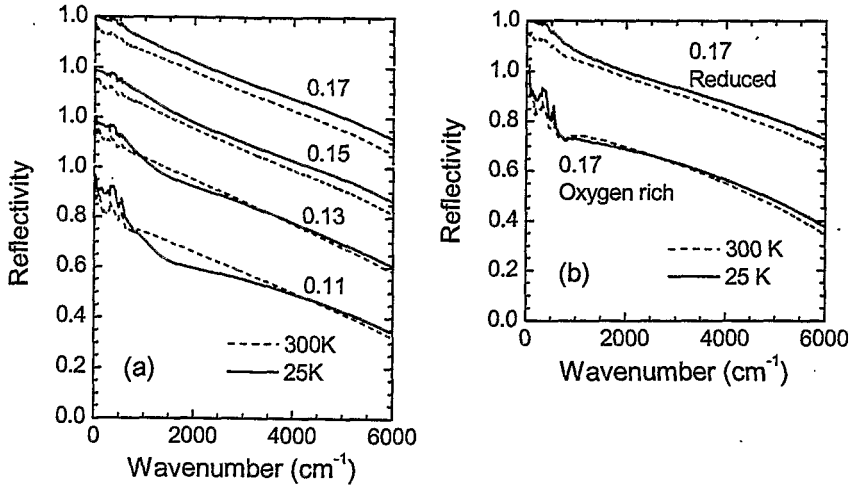

Figure 2. Temperature dependence of the infrared reflectivity for (a) the four University of Maryland films and (b) the reduced and oxygen rich University of Sherbrooke samples. Note that the vertical scale is shifted by 20% for each sample.

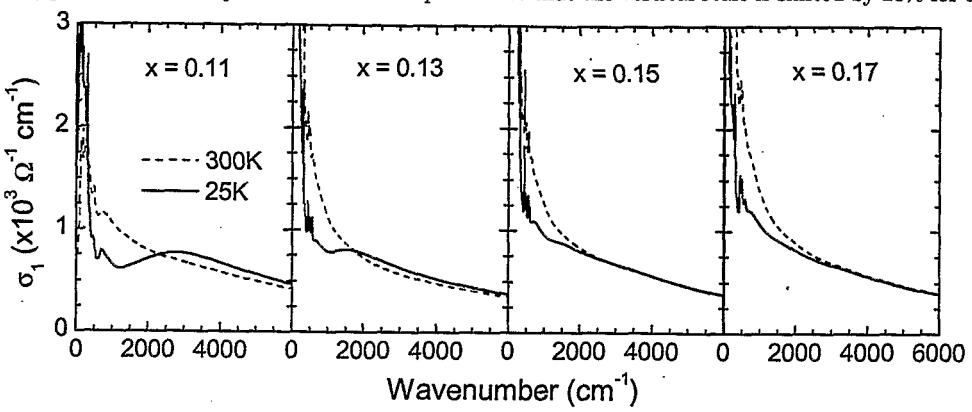

Figure 3. Real part of the optical conductivity of reduced PCCO films at 300 K and the lowest temperature achieved in the normal state.

dielectric function. This extraction process is fully described by Santader-Syro *et al.*[14] Due to the restricted spectral range measured for the Sherbrooke films, we cannot reliably calculate their conductivities. Our analysis for these samples will be based on the reflectivity only.

3. THE NORMAL STATE GAP

The real part of the optical conductivity of the University of Maryland films is shown in Fig. 3. All samples show a low frequency Drude-like peak which narrows with decreasing temperature. Moving up in frequency, one can see a clear dip-hump structure in the $x = 0.11$ and $x = 0.13$ samples, a direct consequence of the feature observed in the reflectivity (Fig. 2). A similar conductivity has also been observed in NCCO crystals.[5,6,15–17] This dip-hump structure is absent from the 0.17 sample and unclear in the 0.15.

To get a better understanding on this feature, it is useful to define a restricted spectral weight as

$$W(\omega_1, \omega_2, T) = \int_{\omega_1}^{\omega_2} \sigma_1(\omega, T) d\omega. \tag{1}$$

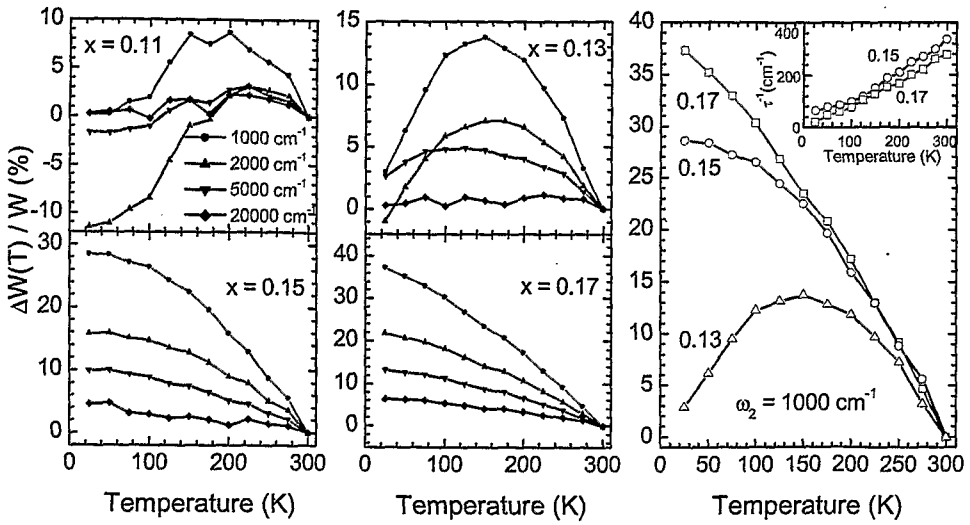

Figure 4. The four left panels show the relative variation of the restricted spectral weight $\Delta W/W = [W(T) - W(300K)]/W(300K)$ for the University of Maryland PCCO films using $\omega_1 = 0$ and four values for ω_2 given in the legend. The right panel compares the data with $\omega_2 = 1000$ cm^{-1} for samples with $x = 0.13$, 0.15 and 0.17. The inset shows the zero frequency extrapolation of the optical scattering rate for the $x = 0.15$ and 0.17 films.

Equation 1 looks at a local change of spectral weight between two cut-off frequencies ω_1 and ω_2, providing some insight into the rearrangement of the conductivity with temperature. The limits $\omega_1 \to 0$ and $\omega_2 \to \infty$ lead to the conventional temperature independent f-sum rule.

Let's consider a conventional metal described by a Drude conductivity with a scattering rate (τ^{-1}) that decreases with decreasing temperature. In this case spectral weight is transfered from high to low energies as T decreases. By taking $\omega_1 = 0$ and $\omega_2 \sim \tau^{-1}$, Eq. 1 implies that W increases at low temperature. Conversely, W should decrease at low temperatures in the case of a gap opening as a consequence of a low to high energy spectral weight transfer.

Figure 4 shows the relative variation of the restricted spectral weight defined as $\Delta W/W = [W(T) - W(300K)]/W(300K)$ for the University of Maryland samples. In all cases we used Eq. 1 with $\omega_1 = 0$ and four different values for the upper cut-off frequency ω_2. As expected from the f-sum rule, increasing ω_2 decreases the magnitude of the temperature variation of $\Delta W/W$ for all samples. Note however, that for the highest doping samples, $\omega_2 = 20000$ cm^{-1} is still not large enough to get rid of all temperature dependence in the restricted spectral weight. When decreasing ω_2 to the 1000–5000 cm^{-1} range, the various samples exhibit very different behaviors. For $x = 0.17$, the spectral weight increases steadily as T decreases to 25 K. This metallic trend is reversed for $x = 0.11$ below 200 K and below 150 K for $x = 0.13$. This slope inversion is the signature of spectral weight being transferred from low to high energy, characteristic of a gap opening. The sample with $x = 0.15$, displays an intermediate behavior as the spectral weight levels off at all ω_2 values. A gap-like feature in this sample is unclear.

To shed some light on this issue, we plot on the right panel of Fig. 4 $\Delta W/W$ for the samples with $x = 0.13$, 0.15 and 0.17 and $\omega_2 = 1000$ cm^{-1}. Cooling from room temperature, all samples show an increase of $\Delta W/W$, consistent with a Drude-like peak narrowing. Around 150 K, the gap opening in the $x = 0.13$ film reverses the trend and the low frequency spectral weigh decreases. Initially, both 0.15 and 0.17 show the same monotonic increase of $\Delta W/W$. However, below about 125 K, the $x = 0.13$ low frequency spectral weight increases slower than that from $x = 0.17$. This effect could be attributed to a different thermal evolution of the Drude-like peak due to scattering rate effects. However, as shown in the inset of this figure, the scattering rate of both samples are almost the same and, most important, there is no feature in the temperature dependence of the $x = 0.15$

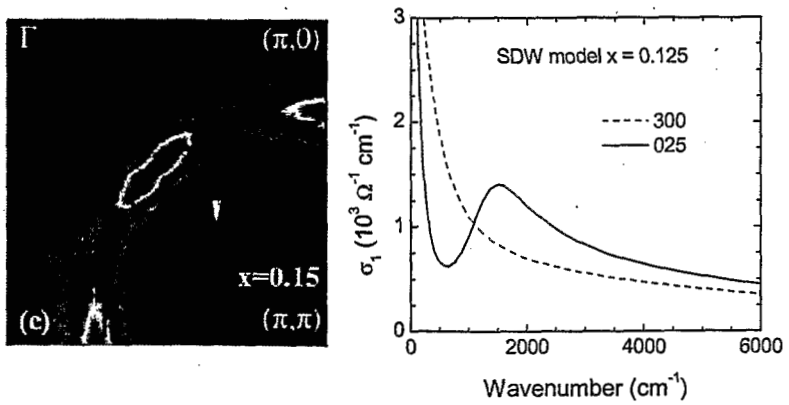

Figure 5. *Left panel:* Fermi surface determined from ARPES by Armitage *et al.*[7] with the solid lines being the Fermi surface expected by the SDW model described in the text. *Right panel:* Optical conductivity at 300 K and 25 K calculated from the SDW model for a nominal Ce concentration of 0.125.

scattering rate. Therefore, the saturation observed in $\Delta W/W$ strongly suggests that a small gap opens below around 100 K for $x = 0.15$. Nevertheless, this gap is only partial, *i.e.*, it does not open over the whole Fermi surface as, for all concentrations, Fig. 3 shows that a Drude-like peak persists at all temperatures.

Neutron scattering consistent with a commensurate (π, π) magnetic order has been unambiguously observed at lower dopings,[18–20] but whether the order exists at superconducting concentrations is not yet settled. To investigate whether this physics explains the gap observed in our experiments we have calculated the optical conductivity of a theoretical model of electrons moving in a band structure defined by the tight-binding dispersion appropriate to the cuprates[21, 22] along with a (π, π) density wave gap of magnitude $2\Delta_{SDW}$ (corresponding to the photoemission band splitting) and mean field $T-$dependence. Our spin density wave model uses the optical matrix elements appropriate to the tight binding model and also includes a frequency and temperature dependent self energy with imaginary part increasing from a T-dependent dc limit [chosen to roughly reproduce $\rho(T)$ at $T < T_W$] to a weakly T-dependent high ω limit. The specific form chosen is $\Sigma(\omega, T) = i\gamma_0 + i\gamma_1 \left[1 - \lambda(T)\omega_c \left(\omega_c - i\omega\right) / (\omega_c^2 + \omega^2)\right]$ with $\gamma_0 = 0.01$ eV, $\gamma_1 = 0.25$ eV, $\omega_c = 0.3$ eV and λ ranging from 0.7 at 300 K to 0.96 at low T. (Note that a 'marginal Fermi liquid' self energy would have described the data almost as well, and leads to results very similar to those presented here.) As discussed by Millis and Drew[22] we also included frequency and matrix element rescalings, by factors ~ 0.6 to account for high energy (Mott) physics. Thus the absolute values of σ should be regarded as estimates, but the relative frequency and temperature dependence as well as spectral weight trends are expected to be reliable.

The left panel of Fig. 5 shows the low temperature NCCO Fermi surface measure by ARPES.[7] The solid line in this figure represents the expected Fermi surface from our SDW calculations. The calculation predicts a Fermi surface that is exactly twice the measured surface. The absent portions of the Fermi surface can be explained in terms of probability transition between these states. In fact more detailed calculations based on magnetic ordering do show these portions of the Fermi surface vanishing.[23] The calculated conductivity, for the doping $x = 0.125$ and a gap which opens at 170 K and saturates at a $T = 0$ value $2\Delta_{SDW} = 0.14$ eV are shown in shown in the right panel of Fig. 5. The resemblance to the measured conductivity (Fig. 3) is striking.

We can therefore use the spectral weight plots of Fig. 4 to define a gap opening temperature and to show that this temperature vanishes for a Ce concentration in the range $0.15 < x < 0.17$. This temperature and the SDW model interpretation yield a phase diagram with a quantum critical point inside the superconducting dome.[8]

4. COMPETITION BETWEEN OXYGEN AND CERIUM DOPING

To verify the magnetic origin for the normal state gap, we looked into the problem of oxygen doping. To achieve a superconducting transition, electron doped cuprates must be thermally treated in reducing atmosphere. The

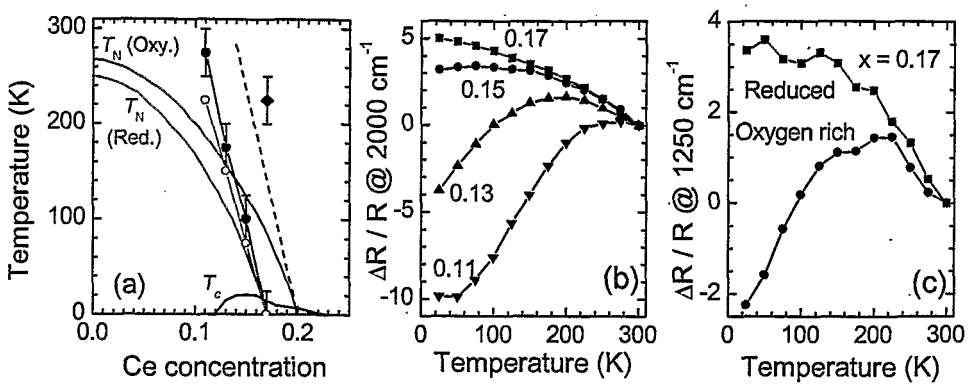

Figure 6. The phase diagram of panel (a) shows the superconducting dome for our reduced PCCO films, the antiferromagnetic phase for reduced and oxygen rich NCCO from Mang *et al.*[10] The solid symbols are the temperatures at which the reflectivities shown in panels (b) and (c) go through a maximum (circles are for Maryland samples and the diamond is for the oxygen rich Sherbrooke film). The open circles are the gap opening temperature determined from the spectral weight analysis for the University of Maryland samples (similar error bars as those for symbols have been omitted for clarity). The dashed line is the expected SDW behavior for the oxygen rich samples obtained by translating the solid line representative of the reduced samples. Panel (b) shows the relative variation of the reflectivity $\Delta R/R = [R(T) - R(300K)]/R(300K)$ for the University of Maryland films at 2000 cm^{-1} and panel (c) shows the same quantity for the University of Sherbrooke films at 1250 cm^{-1}.

reducing level at which the superconducting properties are optimized is situated at the edge of dissociating the material. Interestingly, Mang *et al.* showed that reduction of the sample also moves the antiferromagnetic phase boundary to lower temperatures.[10] In this section we compare the reflectivity of reduced and oxygenated samples and their relation to the antiferromagnetic phase.

As we suggested in the previous section, the normal state gap could have its origins in a SDW ordering. The temperature at which this gap opens can be determined from the low frequency restricted spectral weight. In Fig. 6 (a) we show the phase diagram of electron doped cuprates. This plot shows the antiferromagentic phase boundary measured by neutrons[10] for reduced NCCO. The open circles represent the temperature at which the gap in PCCO opens, as determined by the spectral weight analysis. This picture suggests that the gap could be 2D fluctuations eventually leading to the 3D antiferromagnetic order. If this was the case, changing the Néel temperature should also change our gap opening temperature. This issue can be addressed by looking at oxygen rich samples.

Because of the presently restricted spectral region measured for the oxygen rich sample we cannot calculate its optical conductivity. However, we can estimate the gap opening temperature directly from the reflectivity data. Figure 6 (b) shows the reflectivity of the University of Maryland reduced PCCO samples at 2000 cm^{-1} as a function of temperature. This frequency was chosen to maximize the reflectivity changes with temperature. Note that the curves in Fig. 6 (b) follow a similar behavior as the one observed for the low frequency integrated spectral weight from Fig. 4. We estimated the gap opening temperatures as the maxima in this reflectivity curves. These temperatures are shown as solid circles in Fig. 6 (a). Comparing these points with the open circles, we see that the bare reflectivity tends to overestimate the gap opening temperature by about 20 %, but for the sake of our further analysis, this is not essential.

We then proceeded to the University of Sherbrooke 0.17 films. The evolution of the bare reflectivity at 1250 cm^{-1} is shown in Fig. 6 (c). The reduced sample shows a monotonic increase of the reflectivity with decreasing temperature, consistent with our data for the University of Maryland film. However, the reflectivity of the same 0.17 compound, when oxygenated, shows a maximum in the reflectivity at about 225 K, characteristic of the gap opening. This temperature is plotted in the phase diagram of Fig. 6 (a) as the solid diamond. We also plot the antiferromagnetic phase boundary for non-reduced NCCO.[10] The dashed line is what we would expect for the

gap opening temperature by translating the line obtained for reduced samples. This figure strongly suggests that shifting the Néel temperature also shifts the optical gap opening temperature indicating a relationship between these two phenomena in support of our SDW model.

A final important remark is that although the most clear effect of oxygen doping is to move the antiferromagnetic phase boundary, it should not be interpreted as only an "effective doping". Figure 1 (a) suggests that the behavior expected for our oxygenated 0.17 samples would be somewhere between 0.05 and 0.10. The reflectivity of the 0.17 oxygenated sample says otherwise. In a "effective doping" interpretation, the depth of the dip around 2000 cm^{-1} in its reflectivity should be larger that the one measured for a sample with $x = 0.10$. Comparing the reflectivy of the oxygenated $x = 0.17$ sample to the one for the reduced $x = 0.11$ samples (Fig. 2) we see that this is clearly not the case. This observation is in close agreement with a Hall coefficient that is not negative enough in the oxygen rich $x = 0.17$ films.[13] The gap differences observed between the oxygenated $x = 0.17$ and the reduced $x = 0.11$ samples suggests that oxygen and cerium doping act on different portions of the Fermi surface.

5. CONCLUSIONS

We measured the infrared response of reduced and oxygenated $Pr_{2-x}Ce_xCuO_4$ thin films from room temperature to 25 K. A normal state gap was found in the reduced samples. The gap opening temperature decreases with increasing doping and vanishes between $x = 0.15$ and 0.17. The persistence of a Drude-like peak at all temperatures shows that this gap does not open along the whole Fermi surface, in agreement with ARPES data. This gap reappears in the 0.17 sample when it is oxygen enriched, in close agreement with the changes in the antiferromagnetic phase boundary, supporting our interpretation of a magnetic origin for this normal state gap. However, the effect of oxygenation is not simply to create an "effective doping". The magnitude and shape of the gap observed in the oxygen rich 0.17 material does not agree with the one expected assuming an "effective doping" determined from the resistivity.

ACKNOWLEDGMENTS

The authors thank C.P. Hill and M.C. Barr for help with the films preparation at the University of Maryland. The work at University of Maryland was supported by NSF grant DMR-0352735. The work at Columbia was supported by NSF contract DMR-0338376. Work at Sherbrooke is supported by CIAR, CFI, NSERC (Canada), FQRNT (Québec) and the Fondation de l'Université de Sherbrooke. The work at Brookhaven National Laboratory as supported by DOE under contract DE-AC02-98CH10886.

REFERENCES

1. M.R. Norman, H. Ding, M. Randeria, J.C. Campuzano, T. Yokoya, T. Takeuchi, T. Takahashi, T. Mochiku, K. Kadowaki, P. Guptasarma, and D.G. Hinks, *Nature* **392**, p. 157 (1998).
2. T.P Devereaux, *Phys. Rev. B* **68**, p. 094503 (2003).
3. A.F. Santander-Syro, R.P.S.M. Lobo, N. Bontemps, Z. Konstantinovic, Z.Z. Li and H. Raffy, *Phys. Rev. Lett.* **88**, p. 097005 (2002).
4. A.V. Puchkov, D.N. Basov, and T. Timusk, J. Phys. Condens. Matter **8**, 10049 (1996).
5. Y. Onose, Y. Taguchi, K. Ishizaka, and Y. Tokura, *Phys. Rev. Lett.* **87**, 217001 (2001).
6. Y. Onose, Y. Taguchi, K. Ishizaka, and Y. Tokura, *Phys. Rev. B* **69**, 024504 (2004).
7. N.P. Armitage, F. Ronning, D.H. Lu, C. Kim, A. Damascelli, K.M. Shen, D.L. Feng, H. Eisaki, Z.X. Shen, P. K. Mang, N. Kaneko, M. Greven, Y. Onose, Y. Taguchi, and Y. Tokura, *Phys. Rev. Lett.* **88**, p. 257001 (2002).
8. A. Zimmers, J.M. Tomczak, R.P.S.M. Lobo, N. Bontemps, C.P. Hill, M.C. Barr, Y. Dagan, R.L. Greene, A.J. Millis, and C.C. Homes, *Europhys. Lett.* **70**, p. 225 (2005).
9. Y. Dagan, M.M. Qazilbash, C.P. Hill, V.N. Kulkarni, and R.L. Greene, *Phys. Rev. Lett.* **92**, p. 167001 (2004).
10. P.K. Mang, O.P. Vajk, A. Arvanitaki, J.W. Lynn, and M. Greven, *Phys. Rev. Lett.* **93**, p. 027002 (2004).

11. E. Maiser, P. Fournier, J.L. Peng, F.M. Araujo-Moreira, T. Venkatesan, R. L. Greene, and G. Czjzek, *Physica C* **297**, p. 15 (1998).
12. J.L. Peng, E. Maiser, T. Venkatesan, R.L. Greene, and G. Czjzek, *Phys. Rev. B* **55**, p. R6145 (1997).
13. J. Gauthier, S. Gagné, J. Renaud, M.É. Gosselin, P. Richard, and P. Fournier, *preprint* (2005).
14. A.F. Santander-Syro, R.P.S.M. Lobo, N. Bontemps, W. Lopera, D. Giratá, Z. Konstantinovic, Z.Z. Li, and H. Raffy, *Phys. Rev. B* **70**, 134514 (2004).
15. S. Lupi, P. Maselli, M. Capizzi, P. Calvani, P. Giura, and P. Roy, *Phys. Rev. Lett.* **83**, 4852 (1999).
16. Y. Onose, Y. Taguchi, T. Ishikawa, S. Shinomori, K. Ishizaka, and Y. Tokura, *Phys. Rev. Lett.* **82**, 5120 (1999).
17. E.J. Singley, D.N. Basov, K. Kurahashi, T. Uefuji, and K. Yamada, *Phys. Rev. B* **64**, 224503 (2001).
18. T. R. Thurston, M. Matsuda, K. Kakurai, K. Yamada, Y. Endoh, R. J. Birgeneau, P. M. Gehring, Y. Hidaka, M. A. Kastner, T. Murakami, and G. Shirane , *Phys. Rev. Lett.* **65**, p. 263 (1990).
19. M. Matsuda, Y. Endoh, K. Yamada, H. Kojima, I. Tanaka, R.J. Birgeneau, M.A. Kastner, and G. Shirane, *Phys. Rev. B* **45**, p. 12548 (1992).
20. K. Yamada, K. Kurahashi, Y. Endoh, R.J. Birgeneau, and G. Shirane, *J. Phys. Chem. Sol.* **60**, p. 1025 (1999).
21. O. K. Andersen, A. I. Liechtenstein, O. Jepsen, and F. Paulsen, *J. Phys. Chem. Sol.* **60**, p. 1573 (1995).
22. A.J. Millis and H.D. Drew, Phys. Rev. B **67**, p. 214517 (2003).
23. C. Kusko, R.S. Markiewicz, M. Lindroos, and A. Bansil, *Phys. Rev. B* **66**, p. 140513(R) (2002).